Overview of the torque-controlled humanoid robot TORO

Johannes Englsberger, Alexander Werner, Christian Ott, Bernd Henze, Maximo A. Roa, Gianluca Garofalo, Robert Burger, Alexander Beyer, Oliver Eiberger, Korbinian Schmid, Alin Albu-Schäffer

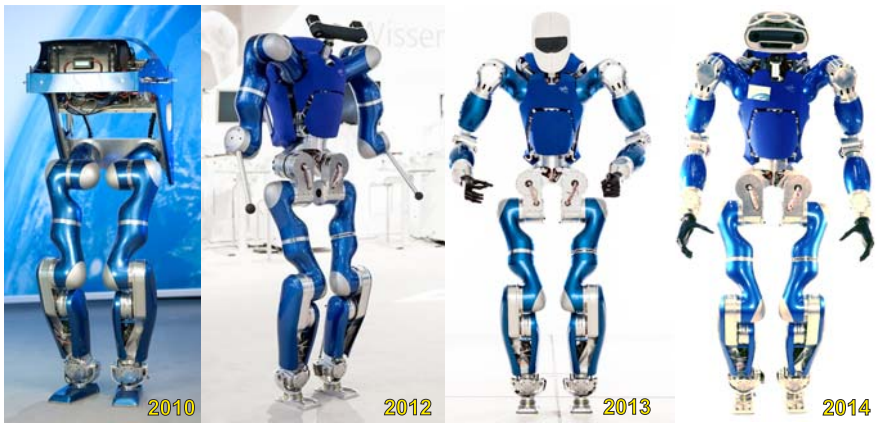

Fig. 1: The torque-controlled humanoid robot TORO and its development stages from 2010 (DLR Biped [1]) to 2014.

***Abstract*— This paper gives an overview on the torque-controlled humanoid robot TORO, which has evolved from the former DLR Biped. In particular, we describe its mechanical design and dimensioning, its sensors, electronics and computer hardware. Additionally, we give a short introduction to the walking and multi-contact balancing strategies used for TORO.**

I. Introduction

Humanoid robotics is an emerging research field with significant potential regarding technological advancement and human prosperity. Humanoid robots aim to reproduce human appearance and capabilities. They can be used to gain deeper understanding on how the human body works. Practical applications include the support of humans, such as in industrial and health-care applications, where the human's working conditions are alleviated by the humanoid robot and productivity is increased. Another use case for humanoid robots is the partial or even full substitution of humans in hazardous situations which may occur during disastrous events or space missions. Compared to other areas of research, the field of humanoid robotics has a relatively short history. Similar to industrial robots, humanoid robots were traditionally based on joint position control, which in combination with a stiff and precisely manufactured drive train leads to a high achievable precision. The first biped robots were developed in Prof. Kato's lab at the University of Waseda. This line of research lead to the development of WABIAN-II [2], the first fully actuated robot which achieved walking with stretched knees. The humanoid robots developed at AIST include HRP-2 [3], which nowadays is used for research in many labs, the dust- and rainproof HRP-3 [4] and HRP-4, a slim walking machine with female shape [5]. The Technical University of Munich developed the walking machines Johnnie [6] and its successor Lola [7], which can achieve high walking speed. Apart from academic research, the developments on biped walking were also largely influenced by company developments like Honda's Asimo [8], Sony's small scale humanoid robot [9], and Toyota's partner robots [10].

Most traditional control strategies rely on very accurate knowledge about the robot dynamics [11]–[14] (i.e. kinematics and inertia properties) and its environment, and work with high-gain joint position control. One of the major breakthroughs in walking control was the introduction of the zero moment point (ZMP) by Vukobratovic [15]. The concept of the ZMP was utilized in the design and control of several impressive biped robots [3], [16]–[18]. The above-mentioned robots belong to the class of electrically driven, fully-actuated walking machines. They are designed as rigid-body systems with only some compliant material in the foot sole for handling the ground impacts during walking.

Recently, torque control for humanoid robots has attracted increased attention. The main expected features - as compared to position control - include robust interaction with the environment and safe and compliant behavior during human robot interaction and in case of self-collisions. Amongst these, the human safety issue probably plays the most crucial role with regard to the use of humanoid robots in the human society [19], [20]. The field of torque control can

 DOI: 10.1109/HUMANOIDS.2014.7041473

be subdivided into several groups. One possible approach is impedance control [21]–[23]. Due to its passivity properties, it is a promising method with regard to human-robot interaction and interaction with an unknown environment. Inverse dynamics control [24]–[26] is another torque-control technique, which provides good tracking capabilities, whilst showing a compliant behavior in case of perturbations.

The increased interest in torque control techniques leads to a demand for physical robots capable of torque sensing and control. In the past few years, several torque-controlled humanoid robots have been realized. Some robots, such as the CB robot [27] and the Petman and Atlas robots by Boston Dynamics Inc. [28] have been implemented based on the principle of hydraulics. One advantage of hydraulics over other actuation principles is its relatively high bandwidth and very high power density. Typical disadvantages of hydraulic humanoids (e.g. Atlas) are their huge power requirements and problems related to noise production (mainly produced by the hydraulic pump). At the same time, the extreme strength of the actuators can be seen as a potential risk regarding human-robot interaction. Additionally, the relatively high and usually unmodeled friction/stiction in hydraulic actuators (as orally reported about Atlas by several DRC teams) can be a challenge with regard to control.

Robots with series elastic actuators form a second prominent group of torque-controlled robots. Here, the torque is measured and indirectly controlled via measurement and regulation of the spring deflection. Some examples of this group of robots are IHMC's M2V2 [29], ETH's StarlETH robot [30], the biped robot Hume [31] from the Human Centered Robotics lab and IIT's COMAN robot [32]. One advantage of series elastic actuators is their mechanical robustness and their shock absorption capabilities (e.g. impacts when walking on rough terrain). Also, when properly controlled [33], series elastic actuation results in high energy efficiency, which can for example increase the maximum achievable traveling distance of biped robots. If the series elastic actuators are highly compliant (i.e. low bandwidth), torque-control techniques cannot be directly applied. In that case, the actuator dynamics has to be considered, which makes the control problem more difficult.

Other robots make use of electrical drive units with torque measurement and control capabilities. When compared to hydraulics, the higher cleanness (no leaking oil) and lower acoustic noise level make it a more convenient solution for research and applications in the human living environment. For some applications, the achievable stiff position control can be advantageous as compared to compliant series elastic actuation. In the past years, DLR has gained expertise with the design and control of torque-controlled electrical robots [1], [21], [22], [34]–[37]. Several generations of Light Weight Robots (LWR) [34] have been developed. They consist of 7 DOF manipulator arms, which can be both position and torque controlled. Based on the LWR technology, both the upper body humanoid robot Justin (2006, [35], enhanced

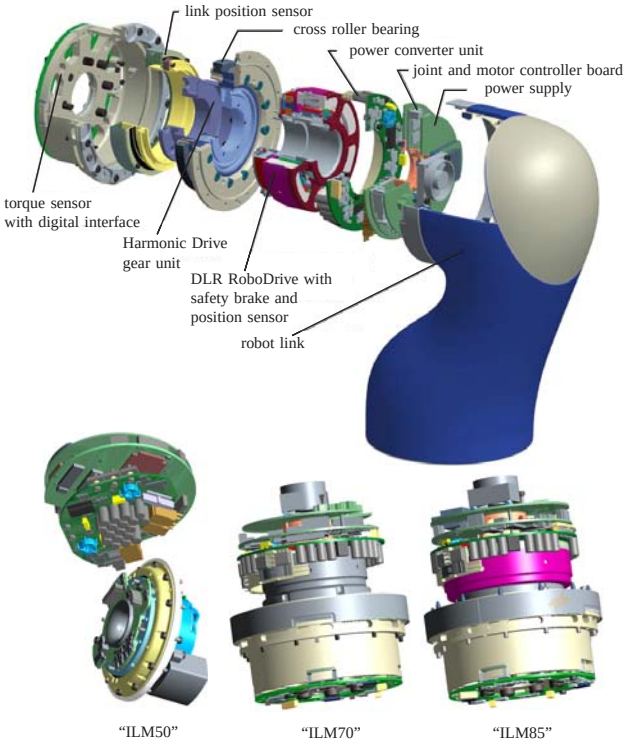

Fig. 2: Light Weight Robot (LWR, [34]) drive unit assembly: top: exploded view; bottom: drive units integrated in TORO.

to Rollin' Justin [36] in 2008) and the DLR Biped robot (in 2010, [1]) were developed. The main focus of (Rollin') Justin is the development of algorithms for advanced manipulation and human-robot interaction. The most prominent design decision concerning the design of DLR Biped was to build it up from the readily available torque-controllable Light Weight Robot (LWR) drive units. Thus, in contrast to other robots that use specifically designed and custom-made drive units [3], [31], [38]–[40], DLR Biped was not designed for fast walking (or even running or jumping). Instead, the mature torque measurement and control capabilities of the LWR drives were exploited without any redesign iteration. This allowed for a very fast development of the robot and gave us access to experimental research in the field of bipedal balancing [41] and walking. We developed Capture Point based walking algorithms [42] and extended them to allow for online footstep replanning (for joystick steering and obstacle avoidance [43]), an increase in walking speed to up to 0.5 $\frac{m}{s}$ [44] and stair climbing (up to 5 cm stair height). After walking and balancing algorithms had reached a mature level, it was decided to widen the robot's field of application to multi-contact balancing, human-humanoid interaction and whole-body manipulation tasks (e.g. carrying a heavy load while walking). Thus, DLR Biped was gradually developed further to the full humanoid robot TORO between 2010 and 2014 (see Fig. 1). The hip and upper body were redesigned and arms, hands and a head were added (again based on

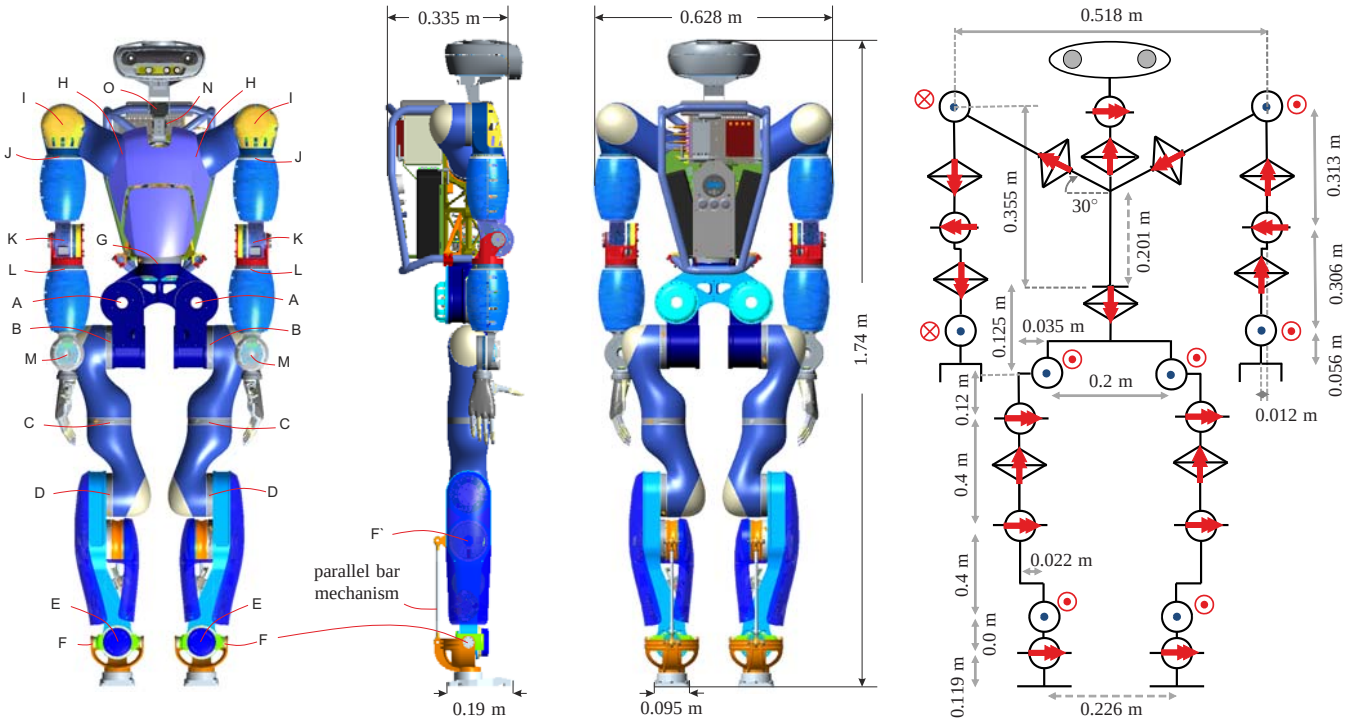

Fig. 3: Overview of TORO's dimensions and joint configuration.

TABLE I: Overview of TORO's joint specifications.

joint	**motor**	**ratio**	$\dot{q}_{max}$	τ_{max}	**range** [°]
A - hip roll	ILM85	160	110 °/s	176 Nm	∓45..±90
B - hip pitch	ILM70	160	157 °/s	100 Nm	-115 .. 90
C - hip yaw	ILM70	160	157 °/s	100 Nm	±120
D - knee	ILM85	100	176 °/s	130 Nm	±105
E - ankle roll	ILM50	160	120 °/s	40 Nm	±19.5
F - ankle pitch	ILM85	100	176 °/s	130 Nm	±45
G - waist	ILM70	160	157 °/s	100 Nm	±120
H - shoulder 1	ILM70	160	157 °/s	100 Nm	±120
I - shoulder 2	ILM70	160	157 °/s	100 Nm	-15..180
J - shoulder 3	ILM50	160	120 °/s	40 Nm	±105
K - elbow	ILM50	160	120 °/s	40 Nm	0..148
L - wrist 1	ILM50	160	120 °/s	40 Nm	-145..118
M - wrist 2	ILM50	160	120 °/s	40 Nm	±105
N - neck yaw	MS106T	225	270 °/s	8.4 Nm	±90
O - neck pitch	MS106T	225	270 °/s	8.4 Nm	-30..90

LWR technology). TORO's main purpose is to serve as an experimental platform for evaluating torque based control approaches. Also, it allows for the comparison of position and torque control techniques for different applications.

The main purpose of this paper is to give an overview of TORO's design. The paper is organized as follows: Section II gives a general overview to TORO's mechanical design and dimensioning. Section III covers TORO's electronics, sensors and computer architecture. In Sec. IV, we shortly outline the control strategies used for walking and multi-contact balancing. Section V concludes the paper.

II. General overview of TORO's design

The main idea followed during the design of TORO was to reuse as many readily available components as possible, in order to accelerate the process of design and putting into operation. In this regard, DLR's experience with the LWR drive units was very beneficial. The drive units including the electronics were all directly used from KUKA[1]-LWR arms.

A. Light Weight Robot drive units

The LWR drive units have a modular design (see Fig. 2) and could thus easily be reused during TORO's design. They include RoboDrive brushless DC motors [46], Harmonic Drive gears, a torque sensor, position sensors (incremental and potentiometer) and a brake system. Additionally, they come with a cross roller bearing that decouples the drive train and the torque sensor from the structural forces and the torques perpendicular to the joint axis. There are three different types of LWR drives: "ILM85", "ILM70" and "ILM50", with a weight (including electronics) of 2.062 kg, 1.678 kg and 0.832 kg, respectively. The gear ratio depends on the chosen Harmonic Drive gear. See table I for their specifications and [46] for further details.

B. Mechanical design and dimensioning

TORO is a human-size humanoid robot with a total height of 174 cm and a weight of 76.4 kg. It has 25 torque-controlled and 2 position-controlled revolute joints

[1]The LWR technology was developed at DLR and transferred to the robotics company KUKA [45], which produces LWR arms in small series.

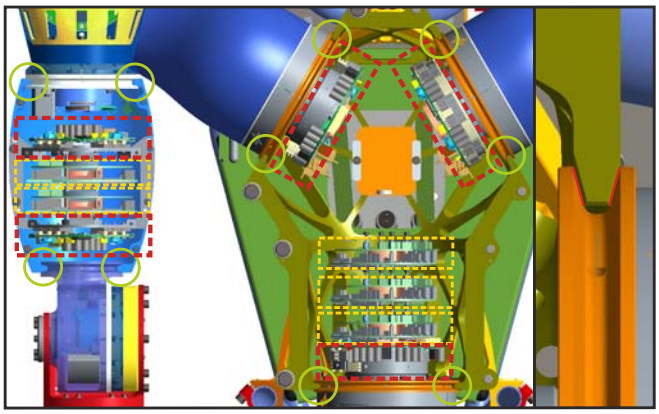

Fig. 4: Wedge mechanism and electronics placing. Motor power-electronics are marked by red rectangles, power supply, joint and motor controller by yellow rectangles. Green circles mark the clamping wedges. Right: detail view of the wedge mechanism. Red marks denote the clamping grooves.

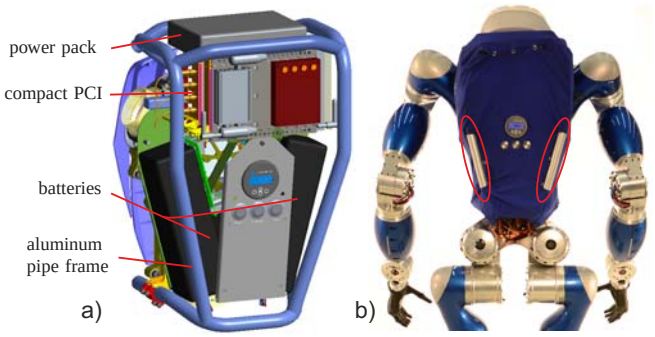

Fig. 5: Backpack, red elliptic markers denote handle bars.

(excluding hand joints): six joints per leg, six joints per arm, one yaw joint in the waist and two position-controlled joints in the neck. Figure 3 gives an overview of its most important dimensions and its joint configuration. We identified the required joint torques and velocities by performing standard motions (e.g. walking, squatting) in OpenHRP simulations and accordingly selected the actuation parameters (i.e. choice of motors and gears). The position-controlled joints are equipped with Dynamixel MS106T servo motors by ROBOTIS Inc. [47]. Table I summarizes TORO's joint specifications. The total weight of 76.385 kg is composed of 21.405 kg from the thorax (including the head), 5.702 kg from each upper arm, 3.813 kg from each lower arm (including hand), 5.617 kg from the hip, 7.648 kg from each thigh and 7.518 kg from each lower leg (including foot).

TORO has gradually evolved from the DLR Biped. With regard to hip design, the DLR Biped had a problem: In some cases (e.g. during stair climbing), it ran into singularity problems as the hip roll and yaw axes were aligned when its knee was lifted high. Thus, the roll-pitch-roll hip configuration from the DLR Biped was redesigned for TORO, such that the three hip axes do not intersect in a single point anymore (see Fig. 3 right). This hip joint configuration allows for a compact hip design and avoids the mentioned singularity problems, as the hip axes can never coincide. Both hip roll joints (**A**) were placed relatively close to the robot's sagittal plane (20 cm apart) to reduce gravitational torque when the robot is standing on one leg. Except for the mentioned changes in the hip configuration, the leg design from the DLR Biped was inherited to TORO. The parallel bar mechanism in TORO's ankle allowed for a relatively slim ankle design and decreased the shanks' inertia. The strong ankle pitch motor (**F'**) is mounted right below the knee, which allows for a comparably slim and strong ankle design (with the given drive units) and decreases the legs' inertia. TORO's feet are flat and comparably small (length: 19 cm, width: 9.5 cm). The foot-size was chosen to allow for full contact with small supporting surfaces (such as short stairs) and to prove the quality of our walking algorithms (see Sec. IV). See [1] for more details about the leg design.

Due to the desired robot proportions, most structural parts from the LWR were replaced by custom-made structural parts. Most of them were milled using Al7075 alloy (an aluminum-based high strength material widely used in aerospace applications). Yet, TORO's thigh and its first shoulder link consist of the structural parts of the KUKA-LWR robot. Due to mechanical requirements and different manufacturing methods used by KUKA, the thigh elements are made of cast aluminum (higher strength) whilst the first shoulder element is made of carbon fiber (lower weight).

TORO's hip, upper body and arms were designed using the exoskeleton principle (as used by nature in insect carapaces, i.e. structural elements consist of outer shells). This allows for very strong and lightweight structures, which support and protect the electronic components. No additional housings are required. The structural elements that form the core part of TORO's thorax are two identical milled aluminum framework parts (see olive-green part in Fig. 4). A wedge based clamping mechanism (clamped via tangential screws; see detail view in Fig. 4 right) is used to connect these structural elements to TORO's arms and waist and form a stiff and strong unit. The sum of TORO's thorax structural parts accounts for only 1.97 kg (excluding backpack pipe).

Just like in the thorax, the structural parts in TORO's arms use the exoskeleton principle and the same wedge clamping mechanism. Their design, as compared to the thorax, is round shaped to create space for the drive electronics (see Fig. 4) and closed to protect the electronics during interaction with the environment and with humans. TORO's arms were designed to have approximately anthropomorphic dimensions and to carry a maximum of 5 kg each. This allows TORO to carry objects with a weight of up to 10 kg and to produce corresponding additional end-effector forces during multi-contact balancing. This design specification was implemented by the choice of two "ILM70" drive unit in TORO's shoulder and four "ILM50" drive units in the remaining

arm. The main focus of the research with TORO is not on dexterous manipulation but rather on balancing and simple manipulation tasks. To provide TORO with a robust solution for picking up simple objects and establishing firm contacts with its environment, it was equipped with electrical hand prostheses (i-limb ultra revolution prosthesis from Touch Bionics [48]). Each finger has one active and one additional passively coupled DOF. The thumbs have one additional DOF, so that they can be opposed to the other fingers. Although the i-limb hands have no position or torque sensors available, they have powerful intrinsic grasping capabilities.

The main part of TORO's computer system and auxiliary electronics (see Sec. III) is located in the backpack (see Fig. 5). It mainly consists of a backplate (which the components are screwed onto), a welded aluminum pipe frame and elastic fabric. The aluminum pipe frame is used as a suspension point for the security rope, as mechanical protection of the backpack's interior and as handle bars (see red markers in Fig. 5b), which are used to manually support the robot after failed experiments. TORO's neck has an actuated pan tilt unit based on the commercially available Dynamixel MS106T servo motors [47]. The structural parts of TORO's head (see Fig. 6) were designed to provide the highest possible stiffness. The head structure contains all required sensors and a computer system for an onboard ego-motion estimation and mapping (see Sec. III-B). This high structural stiffness is not only required for mechanical protection (e.g. when the suspension rope hits the head after a fall), but also to avoid low frequency vibrations of the head, which can cause problems regarding ego-motion estimation.

Throughout the robot, hollow axes are used in the joints to allow for an internal routing of all cables. This avoids the cables from getting caught or tangled.

III. Mechatronics and Computer Hardware

A. Electronics

The same electronics as in the LWR (see Fig. 2) is used to power TORO's joint drives (except for the neck drives). It includes the motor power supply, electronics for motor control, brakes, joint position and torque sensing and control and communication between joint and control computers via Sercos-II bus (see Sec. III-C). The drive units and the electronic components supplying them are mounted as close to each other as possible (see Fig. 4) in order to reduce electromagnetic crosstalk and cable routing.

Two battery packs in TORO's backpack are used to power the robot. They consist of industrial cells based on $LiFePO_4$ and have a nominal voltage of 48 V, a capacity of 6.6 Ah and a weight of 2.3 kg each. These batteries supply power to the joints directly and to the computers via switching mode power supplies. The usual time the robot can operate on a set of batteries is one hour (e.g. walking or whole-body tasks). Alternatively, TORO can be supplied with electricity via a power cable. The power drawn in steady state is approximately 250W. The field of humanoid

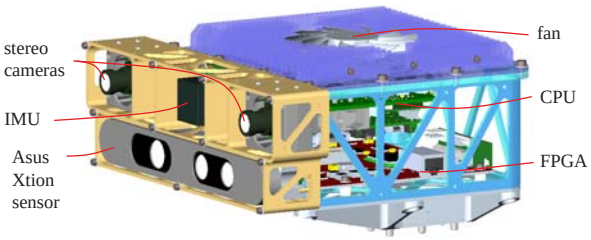

Fig. 6: TORO's head.

robots is currently more focused on capabilities than on power consumption, but endurance is also of high relevance for real-world applications. Taking this perspective, it is interesting to note that when TORO stands still, its power consumption is dominated by its electronics rather than its motors. Thus, in the design of a new humanoid prototype, we would pay special attention to the issue of electrical efficiency. To facilitate good heat dissipation in TORO, the joint drives' power electronics are either directly connected to the structural parts (made of aluminum that provides good heat conduction) or cooled via forced and natural convection.

B. Sensors

Each of the 25 installed LWR drives is equipped with an incremental motor position sensor, an output position sensor and a torque sensor. The torque sensors are mounted on the joint output side. Thus, torque measurements are almost not affected by frictional effects in the joints. Additionally, each joint has a built-in brake, which is activated either by user command or automatically in case of power-down. In this way, the robot's joint positions rarely have to be recalibrated although no precise absolute joint position sensors are available (yet, the ILM70 and ILM85 modules have built-in potentiometers that allow for partially automated recalibration). A recalibration is mainly necessary when a power-down occurs during robot operation and the internally tracked joint position is no longer updated while the joints keep moving (despite engaged brakes) due to the link inertia.

Each of TORO's feet is equipped with a 6 DOF force-torque sensor (FTS), which is mounted directly above the foot. The FTS are used to measure the ground reaction wrenches independently of the robot's leg configuration, and to compute the zero moment point (ZMP), which is necessary for ZMP-based walking algorithms. The FTS are designed to measure forces and torques up to 1000 N and 100 Nm.

An inertial measurement unit (IMU) is mounted to TORO's thorax to measure its orientation and spatial acceleration. TORO's head (see Fig. 6) contains all sensors and the computer system required to estimate the robot's ego-motion and build up a map of its environment.

The sensory information of a pair of stereo cameras is processed on an onboard FPGA using Semi Global Matching (SGM) [49] with a resolution of 0.5 MPixel at a rate of 15 Hz. The resulting depth images and extracted image features are used to calculate delta poses between camera

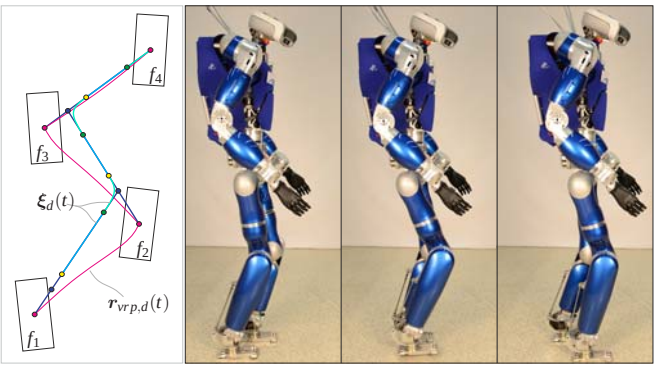

Fig. 7: left: DCM reference $\xi_d(t)$ and nominal VRP trajectories $r_{vrp,d}(t)$ [42]. right: DCM-based walking control.

keyframes. These measurements are fused with IMU measurements in a delayed state Extended Kalman Filter to estimate pose and velocity of the head as well as IMU sensor biases. The depth images are integrated into a 3D environment map [50]. State estimates and map are sent to the real-time control computer in the backpack (profiting from a distributed computing architecture). Additionally, the head comes with an Asus Xtion Pro sensor (which works at 30 fps, [51]) that provides a depth image of the robot in the range of around 0.7 m to 4 m. This depth image is partially redundant to the one computed via stereo cameras and SGM. This redundancy can be exploited to create more robust depth image perception. Especially, bad performance of the Xtion sensor in daylight and inability of a stereo camera system to work in darkness can be compensated with this dual system.

The full integration of the ego-motion estimation from TORO's head into our control framework is part of ongoing work. We also plan to additionally fuse kinematic information into the state estimation process.

C. Computer architecture

Most of TORO's system architecture with regard to joint technology is analog to the Light Weight Robot [34]. All drives apart from the neck are LWR drives, connected via the Sercos-II ring bus and use glass fibers as transmission medium. Thus, the single units are galvanically isolated from each other. The drives provide measurements of joint torque and position and receive a desired position or torque, which are locally controlled by the joint electronics at a 3 kHz rate.

TORO contains two Intel® Core i7® computers. They are located in a compactPCI rack in its backpack (see Fig. 5). One of them is used for real-time control, the other one for high-level planning and communication with drives and sensors. The computers used for the ego-motion estimation and mapping are a Core2Duo and an ARM7 located in the head. The on-board computers are connected via Ethernet, while the off-board workstation (used for supervision and high-level control commands) connects via wireless LAN. To provide a consistent interface towards the various sensors and drives, a hardware abstraction layer (HAL) is used to

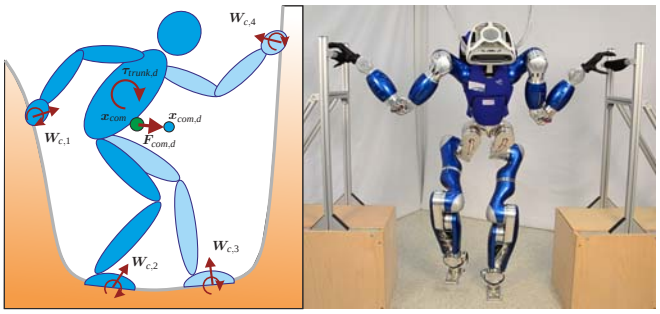

Fig. 8: Wrench distribution and multi-contact balancing

offer interfaces to the control software. For the connection of the software components, a proprietary real-time capable middleware is used. It allows for communication over shared memory and across the network. Introspection and logging of all signals is possible. All hardware interfaces are presented to the controller software through the middleware.

The real-time operating system used on TORO is Real-Time Linux based on Kernel 3.0. The clock of the Sercos-II bus is used to trigger the control loop. The full control loop is operating at a frequency of 1 kHz with a deterministic latency of 2 ms. The sensor data of joint position and torque sensors are available at a 1 kHz rate and the FTS data at a rate of 500 Hz. The real-time control software is developed in Simulink. The Simulink Coder^{TM} (a.k.a. Real-Time Workshop) is used to generate C Code, which is then compiled and uploaded to the robot. Simulink's built-in "external mode" control mode is used as user interface.

IV. Control Strategies

This section provides an overview of the walking and balancing controllers implemented in TORO. The video in [52] illustrates their performance and provides an overview of additional applications of TORO.

A. DCM-based walking

The walking algorithms used for TORO are based on the Divergent Component of Motion (DCM, a.k.a. "Capture Point" [53]). Recently [54], [55], we extended this method to 3D and derived methods to guarantee continuous leg forces during double support and heel-to-toe shift. In 3D, the Divergent Component of Motion (DCM) is defined as

$$\boldsymbol{\xi} = \boldsymbol{x} + b\,\dot{\boldsymbol{x}}, \tag{1}$$

where $\boldsymbol{\xi} = [\xi_x, \xi_y, \xi_z]^T$ is the DCM, $\boldsymbol{x} = [x, y, z]^T$ and $\dot{\boldsymbol{x}} = [\dot{x}, \dot{y}, \dot{z}]^T$ are the CoM position and velocity and $b > 0$ is the time-constant of the DCM dynamics. The naturally stable CoM dynamics can be found by reordering:

$$\dot{\boldsymbol{x}} = -\frac{1}{b}\,(\boldsymbol{x} - \boldsymbol{\xi}). \tag{2}$$

Thus, the CoM automatically (by definition) follows the DCM. Our method makes use of the so called *Enhanced Centroidal Moment Pivot point* (eCMP), which encodes the

external (e.g. leg-) forces in a linear force law and the *Virtual Repellent Point* (VRP), which encodes the total force acting on the CoM (external plus gravitational force). Both eCMP and VRP are "invariant force application points" [56], which facilitate the design of force profiles for dynamic locomotion. Using the VRP, the DCM dynamics can be expressed as

$$\dot{\boldsymbol{\xi}} = \frac{1}{b}\,(\boldsymbol{\xi} - \boldsymbol{r}_{vrp}). \tag{3}$$

The simple DCM dynamics is exploited to generate a DCM reference trajectory ($[\boldsymbol{\xi}_d, \dot{\boldsymbol{\xi}}_d]$, see Fig. 7 left), which is tracked via the following feed-back controller:

$$\boldsymbol{r}_{vrp,c} = \boldsymbol{\xi} + k_\xi\, b\,(\boldsymbol{\xi} - \boldsymbol{\xi}_d) - b\,\dot{\boldsymbol{\xi}}_d. \tag{4}$$

The desired VRP $\boldsymbol{r}_{vrp,c}$ is then transformed into a corresponding desired leg force $\boldsymbol{F}_{leg,c}$ via

$$\boldsymbol{F}_{leg,c} = \frac{mg}{\Delta z_{vrp}}\,(\boldsymbol{x} - (\underbrace{\boldsymbol{r}_{vrp,c} - \begin{bmatrix}0 & 0 & \Delta z_{vrp}\end{bmatrix}^T}_{\boldsymbol{r}_{ecmp,c}})), \tag{5}$$

where m is the robot's mass, g is the gravitational constant and Δz_{vrp} can be interpreted as "average CoM height". The brace indicates the correlation between eCMP and VRP. Our walking algorithm is currently based on admittance control, which has disadvantages in case of interaction with the environment. Embedding DCM control into an inverse dynamics based whole-body control framework - with better compliance properties - is part of our ongoing research. Fig. 7 (right) shows an example of DCM-based walking.

B. Multi-contact balancing

The extension of the torque-based balancing and posture controller from [41] (originally derived for bipedal robots) to multi-contact balancing is part of our current research and will be shortly outlined in the following: Given a desired equilibrium $\boldsymbol{x}_{com,d}$ for the CoM position and a desired orientation $\boldsymbol{R}_d$ of the hip, we compute a desired wrench $\boldsymbol{W}_d$ that we want to apply at the robot's CoM according to a compliance control law in the form of

$$\boldsymbol{W}_d = \begin{bmatrix} m\boldsymbol{g} \\ 0 \end{bmatrix} - \boldsymbol{D}\begin{bmatrix} \dot{\boldsymbol{x}}_{com} \\ \boldsymbol{\omega} \end{bmatrix} - \begin{bmatrix} \boldsymbol{K}(\boldsymbol{x}_{com} - \boldsymbol{x}_{com,d}) \\ \boldsymbol{\tau}_k(\boldsymbol{R}, \boldsymbol{R}_d) \end{bmatrix} \tag{6}$$

where $\boldsymbol{R}$ and $\boldsymbol{\omega}$ denote the orientation and the angular velocity of the hip, which are both measured by an onboard IMU. $\boldsymbol{D}$ is a damping matrix. $\boldsymbol{K}$ denotes the translational stiffness and $\boldsymbol{\tau}_k$ the torque from a virtual rotational spring between $\boldsymbol{R}$ and $\boldsymbol{R}_d$. The desired wrench $\boldsymbol{W}_d$ is distributed to desired contact wrenches $\boldsymbol{W}_{c,i}$ acting at the i end-effectors that are currently in contact (see Fig. 8). The used method is based on solving a quadratic optimization problem (QP), which includes inequality constraints regarding friction, unilaterality of contact forces and limitations for the center of pressure (CoP). The optimization generates a Cartesian impedance for all the end-effector directions which are not used for balancing. The desired end-effector wrenches are mapped quadi-statically via a Jacobian transpose to the joint torques, which are commanded to the robot.

V. Conclusion and Future Research Topics

In this paper, we gave an overview on TORO, a torque-controlled humanoid robot, which has evolved from the former DLR Biped robot [1] (see Fig. 1). TORO's dimensioning, mechanical design and mechatronics (including electronics, sensors and computer architecture) were described. Additionally, we shortly described the strategies used for walking and multi-contact balancing. In retrospect, we believe that TORO is a reliable platform for basic research on torque-based whole-body control including walking, balancing and physical interaction with humans and the environment. We had decided to build up TORO from the readily available LWR drive units, which led to restrictions regarding high performance tasks (e.g. fast walking and running, deep squats, climbing high stairs). In this regard, we expect that the insights gained during the work with TORO will be very beneficial for the design of next-generation humanoid robots.

Our future intended research topics include inverse dynamics and impedance based walking and whole-body control, safe human-humanoid interaction, humanoid-based telepresence and the design of further humanoid prototypes.

Acknowledgements

The authors want to thank all colleagues and the staff from DLR's electrical and mechanical workshops involved in the process of developing and manufacturing TORO.

This research is partly supported by the Initiative and Networking Fund of Helmholtz Association through a Helmholtz Young Investigators Group (Grant no. VH-NG-808).

References

[1] C. Ott, C. Baumgärtner, J. Mayr, M. Fuchs, R. Burger, D. Lee, O. Eiberger, A. Albu-Schäffer, M. Grebenstein, and G. Hirzinger, "Development of a biped robot with torque controlled joints," in *IEEE-RAS Int. Conf. on Humanoid Robots*, 2010, pp. 167–173.

[2] Y. Ogura, H. Aikawa, K. Shimomura, H. Kondo, A. Morishima, H. ok Lim, and A. Takanishi, "Development of a new humanoid robot WABIAN-2," in *IEEE Int. Conf. on Robotics and Automation*, 2006.

[3] K. Kaneko, F. Kanehiro, S. Kajita, H. Hirukawa, T. Kawasaki, M. Hirata, K. Akachi, and T. Isozumi, "Humanoid robot HRP-2," in *IEEE Int. Conf. on Robotics and Automation*, 2004, pp. 1083–1090.

[4] K. Kaneko, K. Harada, F. Kanehiro, G. Miyamori, and K. Akachi, "Humanoid robot HRP-3," in *IEEE/RSJ Int. Conf. on Intell. Robots and Systems*, 2008, pp. 2471–2478.

[5] K. Kaneko, F. Kanehiro, M. Morisawa, K. Miura, and S. N. S. Kajita, "Cybernetic human HRP-4C," in *IEEE-RAS Int. Conf. on Humanoid Robots*, 2009, pp. 7–14.

[6] M. Gienger, K. Löffler, and F. Pfeiffer, "Design and control of a biped walking and jogging robot," in *2nd Int. Conf. on Climbing and Walking Robots (CLAWAR)*, 1999.

[7] S. Lohmeier, T. Buschmann, and H. Ulbrich, "System design and control of anthropomorphic walking robot LOLA," *IEEE/ASME Transactions on Mechatronics*, vol. 14, no. 6, pp. 658–666, 2009.

[8] Y. Sakagami, R. Watanabe, C. Aoyama, S. Matsunaga, N. Higaki, and K. Fujimura, "The intelligent ASIMO: system overview and integration," in *IEEE/RSJ Int. Conf. on Intell. Robots and Systems*, 2002, pp. 2478–2483.

[9] T. Ishida, Y. Kuroki, and J. Yamaguchi, "Mechanical system of a small biped entertainment robot," in *IEEE/RSJ Int. Conf. on Intell. Robots and Systems*, 2003, pp. 1129–1134.

[10] R. Tajima, D. Honda, and K. Suga, "Fast running experiments involving a humanoid robot," in *IEEE Int. Conf. on Robotics and Automation*, 2009, pp. 1571–1576.

[11] Y. Choi, D. Kim, and B.-J. You, "On the walking control for humanoid robot based on the kinematic resolution of CoM jacobian with embedded motion," in *IEEE Int. Conf. on Robotics and Automation*, 2006.

[12] S. Kajita, M. Morisawa, K. Miura, S. Nakaoka, K. Harada, K. Kaneko, F. Kanehiro, and K. Yokoi, "Biped walking stabilization based on linear inverted pendulum tracking," in *IEEE/RSJ Int. Conf. on Intell. Robots and Systems*, 2010, pp. 4489–4496.

[13] T. Takenaka, T. Matsumoto, and T. Yoshiike, "Real time motion generation and control for biped robot, 1st report: Walking gait pattern generation," in *IEEE/RSJ Int. Conf. on Intell. Robots and Systems*, 2009, pp. 1084–1091.

[14] J. Urata, K. Nishiwaki, Y. Nakanishi, K. Okada, S. Kagami, and M. Inaba, "Online decision of foot placement using singular LQ preview regulation." in *IEEE-RAS Int. Conf. on Humanoid Robots*, 2011.

[15] M. Vukobratovic and Y. Stepanenko, "On the stability of anthropomorphic systems," *Mathematical Biosciences*, vol. 15, pp. 1–37, 1972.

[16] K. Hirai, M. Hirose, Y. Haikawa, and T. Takenaka, "The Development of Honda Humanoid Robot," in *IEEE Int. Conf. on Robotics and Automation*, 1998.

[17] I. Park, J. Kim, J. Lee, and J. Oh, "Mechanical design of the humanoid robot platform, HUBO," *Advanced Robotics*, vol. 21, no. 11, 2007.

[18] B. You, Y. Choi, M. Jeong, D. Kim, Y. Oh, C. Kim, J. Cho, M. Park, and S. Oh, "Network-based humanoids Mahru and Ahra," in *Int. Conf. on Ubiquitious Robots and Ambient Intelligence*, 2005, pp. 376–379.

[19] S. Haddadin, S. Parusel, R. Belder, and A. Albu-Schäffer, "It is (almost) all about human safety: A novel paradigm for robot design, control, and planning." in *Int. Conf. on Computer Safety, Reliability and Security*, 2013, pp. 202–215.

[20] S. Haddadin, "Towards Safe Robots - Approaching Asimov's 1st Law," in *Springer Tracts in Advanced Robotics*, 2014, pp. 1–343.

[21] A. Albu-Schaeffer, O. Eiberger, M. Grebenstein, S. Haddadin, C. Ott, T. Wimboeck, S. Wolf, and G. Hirzinger, "Soft robotics: From torque feedback controlled lightweight robots to intrinsically compliant systems," *Robotics and Automation Magazine*, 2008.

[22] C. Ott, A. Albu-Schäffer, A. Kugi, and G. Hirzinger, "On the passivity based impedance control of flexible joint robots," *IEEE Transactions on Robotics*, vol. 24, no. 2, pp. 416–429, 2008.

[23] C. Ott, R. Mukherjee, and Y. Nakamura, "Unified impedance and admittance control," in *IEEE Int. Conf. on Robotics and Automation*, 2010.

[24] J. Buchli, M. Kalakrishnan, M. Mistry, P. Pastor, and S. Schaal, "Compliant quadruped locomotion over rough terrain," in *IEEE/RSJ Int. Conf. on Intell. Robots and Systems*, 2009, pp. 814–820.

[25] M. Mistry, J. Buchli, and S. Schaal, "Inverse dynamics control of floating base systems using orthogonal decomposition," in *IEEE Int. Conf. on Robotics and Automation*, 2010, pp. 3406–3412.

[26] L. Righetti, J. Buchli, M. Mistry, M. Kalakrishnan, and S. Stefan, "Optimal distribution of contact forces with inverse dynamics control," *Int. J. of Robotics Research*, vol. 32, no. 3, pp. 280–298, 2013.

[27] G. Cheng, S.-H. Hyon, J. Morimoto, A. Ude, G. Colvin, W. Scroggin, and S. C. Jacobsen, "CB: A humanoid research platform for exploring neuroscience," in *IEEE-RAS Int. Conf. on Humanoid Robots*, 2006.

[28] "Atlas - the agile anthropomorphic robot." [Online]. Available: http://www.bostondynamics.com/robot_Atlas.html

[29] J. Pratt and B. Krupp, "Design of a bipedal walking robot," in *Proceedings of the 2008 SPIE*, vol. 6962, 2008.

[30] M. Hutter, C. Gehring, M. Bloesch, M. Hoepflinger, C. D. Remy, and R. Siegwart, "Starleth: A compliant quadrupedal robot for fast, efficient, and versatile locomotion," in *15th Int. Conf. on Climbing and Walking Robot-CLAWAR*, 2012.

[31] M. Slovich, N. Paine, K. Kemper, A. Metzger, A. Edsinger, J. Weber, and L. Sentis, "Hume: A bipedal robot for human-centered hyper-agility," in *Dynamic Walking conference*, 2012. [Online]. Available: http://www.me.utexas.edu/ lsentis/files/DW-2012-abstract-3.pdf

[32] N. G. Tsagarakis, S. Morfey, G. Medrano Cerda, L. Zhibin, and D. G. Caldwell, "Compliant humanoid COMAN: Optimal joint stiffness tuning for modal frequency control," in *IEEE Int. Conf. on Robotics and Automation*, 2013, pp. 673–678.

[33] P. Kormushev, B. Ugurlu, S. Calinon, N. Tsagarakis, and D. Caldwell, "Bipedal walking energy minimization by reinforcement learning with evolving policy parameterization," in *IEEE/RSJ Int. Conf. on Intell. Robots and Systems*, 2011, pp. 318–324.

[34] G. Hirzinger, N. Sporer, A. Albu-Schäffer, M. Hähnle, R. Krenn, A. Pascucci, and M. Schedl, "DLR's torque-controlled light weight robot III - are we reaching the technological limits now?" in *IEEE Int. Conf. on Robotics and Automation*, 2002, pp. 1710–1716.

[35] Ch. Ott, O. Eiberger, W. Friedl, B. Bäuml, U. Hillenbrand, Ch. Borst, A. Albu-Schäffer, B. Brunner, H. Hirschmüller, S. Kielhöfer, R. Konietschke, M. Suppa, T. Wimböck, F. Zacharias, and G. Hirzinger, "A humanoid two-arm system for dexterous manipulation," in *IEEE-RAS Int. Conf. on Humanoid Robots*, 2006, pp. 276–283.

[36] C. Borst, T. Wimböck, F. Schmidt, M. Fuchs, B. Brunner, F. Zacharias, P. R. Giordano, R. Konietschke, W. Sepp, S. Fuchs, C. Rink, A. Albu-Schäffer, and H. Gerd, "Rollin'justin-mobile platform with variable base." in *IEEE Int. Conf. on Robotics and Automation*, 2009.

[37] A. Dietrich, T. Wimböck, A. Albu-Schäffer, and G. Hirzinger, "Reactive whole-body control: Dynamic mobile manipulation using a large number of actuated degrees of freedom," *IEEE Robotics & Automation Magazine*, vol. 19, no. 2, pp. 20–33, 2012.

[38] S. Lohmeier, T. Buschmann, H. Ulbrich, and F. Pfeiffer, "Humanoider laufroboter LOLA," in *Tagungsband ROBOTIK 2008*.

[39] J. Urata, Y. Nakanishi, K. Okada, and M. Inaba, "Design of high torque and high speed leg module for high power humanoid," in *IEEE/RSJ Int. Conf. on Intell. Robots and Systems*, 2010, pp. 4497–4502.

[40] N. Paine, S. Oh, and L. Sentis, "Design and control considerations for high-performance series elastic actuators," *Mechatronics, IEEE/ASME Transactions on*, vol. 19, no. 3, pp. 1080–1091, 2014.

[41] C. Ott, M. A. Roa, and G. Hirzinger, "Posture and balance control for biped robots based on contact force optimization," in *IEEE-RAS Int. Conf. on Humanoid Robots*, 2011, pp. 26–33.

[42] J. Englsberger, C. Ott, and A. Albu-Schäffer, "Three-dimensional bipedal walking control using divergent component of motion," in *IEEE/RSJ Int. Conf. on Intell. Robots and Systems*, 2013.

[43] N. Perrin, C. Ott, J. Englsberger, O. Stasse, F. Lamiraux, and D. G. Caldwell, "A continuous approach to legged locomotion planning." [Online]. Available: http://hal.inria.fr/docs/00/80/59/81/PDF/continuous_locomotion_perrin.pdf

[44] H. Kaminaga, J. Englsberger, and C. Ott, "Kinematic optimization and online adaptation of swing foot trajectory for biped locomotion," in *IEEE-RAS Int. Conf. on Humanoid Robots*, 2012, pp. 593–599.

[45] "KUKA Roboter GmbH." [Online]. Available: http://www.kuka-robotics.com

[46] "TQ - Technology in Quality. Fused with former Robodrive GmbH." [Online]. Available: http://www.tq-group.com/en/products/product-details/prod/leichtbau-torque-servomotoren/extb/Main/

[47] "Robotis inc." [Online]. Available: http://www.robotis.com/xe/

[48] "Touch Bionics Inc. - provider of world-leading prosthetic technologies." [Online]. Available: http://www.touchbionics.com/products/i-limb-ultra-revolution

[49] H. Hirschmuller, "Stereo processing by semiglobal matching and mutual information," *Pattern Analysis and Machine Intelligence, IEEE Transactions on*, vol. 30, no. 2, pp. 328–341, 2008.

[50] K. Schmid and H. Hirschmüller, "Stereo vision and imu based real-time ego-motion and depth image computation on a handheld device," in *Robotics and Automation (ICRA), 2013 IEEE International Conference on*, 2013.

[51] "Xtion by ASUSTeK COMPUTER INC." [Online]. Available: https://www.asus.com/de/Multimedia/Xtion_PRO_LIVE/

[52] B. Henze, A. Werner, M. A. Roa, G. Garofalo, J. Englsberger, and C. Ott, "Control applications of TORO - a torque controlled humanoid robot (video)," in *IEEE-RAS Int. Conf. on Humanoid Robots*, 2014.

[53] J. Pratt, J. Carff, S. Drakunov, and A. Goswami, "Capture point: A step toward humanoid push recovery," in *IEEE-RAS Int. Conf. on Humanoid Robots*, 2006, pp. 200–207.

[54] J. Englsberger, C. Ott, and A. Albu-Schäffer, "Three-dimensional bipedal walking control using divergent component of motion," in *IEEE/RSJ Int. Conf. on Intell. Robots and Systems*, 2013.

[55] J. Englsberger, T. Koolen, S. Bertrand, J. Pratt, C. Ott, and A. Albu-Schäffer, "Trajectory generation for continuous leg forces during double support and heel-to-toe shift based on divergent component of motion," in *IEEE/RSJ Int. Conf. on Intell. Robots and Systems*, 2014.

[56] M. B. Popovic, A. Goswami, and H. Herr, "Ground reference points in legged locomotion: Definitions, biological trajectories and control implications," *Int. J. of Robotics Research*, vol. 24, no. 12, 2005.